Nuclear Materials and Energy 38 (2024) 101586

Contents lists available at ScienceDirect

Nuclear Materials and Energy

journal homepage: www.elsevier.com/locate/nme

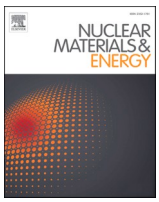

Determination of Tritium-Helium-3 differential cross-section in the energy range between 0.6 MeV and 3.3 MeV for tritium depth profiling in solids

S. Markelj [a,*], A. Cvetinović [a], M. Lipoglavšek [a], M. Kelemen [a], M. Čekada [a], P. Pelicon [a], M. Payet [b], C. Grisolia [b]

[a] Jožef Stefan Institute, Jamova cesta 39, 1000 Ljubljana, Slovenia
[b] CEA, IRFM, F-13108 Saint Paul Lez Durance, Cadarache, France

ARTICLE INFO

Keywords:
Tritium
Helium-3
Nuclear reaction analysis
Differential cross-section

ABSTRACT

The differential cross-section for the ^{3}He+^{3}H nuclear reaction was measured in a thin tritiated PdTi film that was deposited on a Si wafer. The sample was loaded with $^{3}H_2$ gas at a temperature of 300 °C and at a pressure of 1.8 bar. The total activity of the sample, measured by the liquid scintillation technique, was found to be 395 MBq. Two peaks were observed in the spectrum of the thick Si detector, corresponding to the ^{3}H(^{3}He,d)^{4}He and ^{3}H(^{3}He,p)^{5}He reaction channels. The differential cross-section was determined for the energy range of the ^{3}He beam from 0.6 to 3.4 MeV, at three scattering angles of 125, 135 and 155°. The differential cross-section for the first channel remained almost constant within the measured energy range, while the cross-section for the second channel increased with energy. In both cases, the cross-sections reached their maximum value at the lowest scattering angle measured. The differential cross-sections were verified using a thick solid tritiated tungsten target. For assessing the tritium depth profile, only the reaction channel ^{3}H(^{3}He,d)^{4}He can be utilized.

Introduction

Nuclear power plants, especially fusion devices and future GEN IV reactors generate various amounts of tritium (^{3}H), the heaviest and radioactive hydrogen isotope. Due to high-temperature operation conditions, tritium could permeate through the confinement materials and consequently be released into the environment. For this reason, the development of new methods to assess the tritium inventory are essential to evaluate the correct measures for radioactive waste management and to prevent possible emissions to the environment. Techniques for in-situ measurements of tritium concentrations are scarce, so their qualitative and quantitative development, should be the primary objective in order to achieve adequate management of radioactive waste produced in nuclear fusion and fission facilities.

Ion beam methods are among the few techniques that can detect hydrogen isotopes [1], so they are often used for post-mortem analysis of samples exposed to fuel in fusion devices [2]. The elastic recoil detection analysis (ERDA) method [3,4] is often used because it allows the detection of all hydrogen isotopes simultaneously and has a sensitivity for tritium detection of about 10^{15} at./cm^{2} [4]. The disadvantage of the ERDA technique is its sensitivity to surface roughness, as the probing beam hits the surface at shallow angles. In contrast to ERDA, nuclear reaction analysis (NRA) method is typically used for samples with small amounts of hydrogen isotopes due to its high sensitivity [5] and its insensitivity to sample surface roughness and contamination [6,7]. To the authors' knowledge the following nuclear reactions: ^{3}H(^{12}C,p)^{14}C [7], ^{3}H(p,n)^{3}He [8,9] and ^{3}H(d,n)^{4}He [10,11] were utilized for tritium detection by NRA. However, there are several technical difficulties associated with the detection of ^{3}H using these nuclear reactions. Namely, for the second reaction to be used, neutrons must be detected in the time-of-flight regime [9], which is not trivial in conventional ion beam laboratories. The problem with the third reaction is that it produces high neutron yields and the detection of α particles makes it more surface sensitive [8]. In addition, the deuterium (^{2}H) ion beam is not allowed to be used in many laboratories because it produces an intense flux of high energy neutrons that reach radiation safety limits.

There are also other methods such as the accelerator mass spectrometry (AMS) and full combustion method (FCM), which can provide quantitative tritium profiles and are proven to have better detection sensitivity compared to ion beam analysis methods [12]. In addition, chemical etching and subsequent analysis of tritium in the etching solution by liquid scintillation counting can also provide quantitative

* Corresponding author.
E-mail address: sabina.markelj@ijs.si (S. Markelj).

https://doi.org/10.1016/j.nme.2024.101586
Received 17 October 2023; Received in revised form 3 January 2024; Accepted 5 January 2024
Available online 6 January 2024

tritium depth profiling [13,14]. These methods were successfully used to determine very low levels of tritium in samples exposed in the JET fusion device [13,12] and gave very valuable information on the tritium retention. However, it must be emphasised that all these methods are destructive, whereas ion beam methods are in most cases non-destructive. At present, no ion beam method could surpass the tritium sensitivity of the above listed (destructive) methods.

The purpose of this study is to evaluate the cross-section for the nuclear reaction between tritium and ^{3}He. The advantage of using ^{3}He as the primary beam for tritium concentration measurements is that it would allow the detection of tritium simultaneously with deuterium [15,16] and other impurities that are typically present in fission and, especially, fusion environment [2], such as carbon [17], oxygen [18], boron and beryllium [19]. This is important for post-mortem analysis of samples and tiles exposed in fusion devices such as JET and future fusion devices like ITER and DEMO.

In the literature one can find that ^{3}He induces nuclear reactions with tritium, via at least three reaction channels [20,21,22]:

$$^3\mathrm{H} + {}^3\mathrm{He} \rightarrow {}^4\mathrm{He} + {}^2\mathrm{H} + 14.32\ \mathrm{MeV} \quad (1)$$

$$\rightarrow {}^4\mathrm{He} + {}^1\mathrm{H} + \mathrm{n} + 12.09\ \mathrm{MeV} \quad (2)$$

$$\rightarrow {}^5\mathrm{He} + {}^1\mathrm{H} + 11.36\ \mathrm{MeV} \quad (3)$$

$$^5\mathrm{He} \rightarrow {}^4\mathrm{He} + \mathrm{n} + 0.73\ \mathrm{MeV}$$

The listed energies for excess energy values are calculated from updated mass tables [23]. In our last publication [24], a thick solid tritiated W sample was produced in order to probe the efficiency of tritium detection with a ^{3}He ion beam using NRA. An extensive literature search showed that there are only a few measurements done more than sixty years ago with the highest beam energy of 1521 keV [21,22,25]. An overview of the available literature and measured cross-sections is given in [24]. It was shown that the cross-section increases with impact energy and reaches a value of about 2.2 mb/sr at 1087 keV ^{3}He energy at an angle of 90° in the center-of-mass system. Just for comparison, the differential cross-section for the ^{3}He+^{2}H nuclear reaction reaches its maximum of 59.4 mb/sr at the energy of 610 keV at an angle of 135° in the laboratory system [16].

In [24] the comparison of the deuterated and tritiated thick W sample showed that the reaction products with energies in the range from 6.5 to 9.75 MeV are only present in the tritiated sample and not in the deuterated one. This proved that the NRA signal in this energy range is produced by the ^{3}He+^{3}H nuclear reaction (more precisely, from the ^{3}H(^{3}He,d)^{4}He and ^{3}H(^{3}He,p)^{5}He reaction channels). The detected signal increased with ^{3}He energy up to 3.4 MeV and decreased at the highest beam energies. At higher energies, particles coming from the nuclear reaction of the ^{3}He beam with W and target impurities start to interfere with the measurements. Due to the very low signal at individual ^{3}He energies, the quantification of the differential cross-section was not possible in this first attempt [24]. For proper quantification, a more pronounced and better separation of the two peaks coming from the ^{3}H(^{3}He,d)^{4}He and ^{3}H(^{3}He,p)^{5}He channels should be achieved. This could be achieved by using a thinner target with a much higher tritium concentration. Such requirements are achieved in this study using a PdTi thin layer film deposited on a Si wafer. The compound nucleus in the reaction studied is ^{6}Li, which is an interesting nucleus from the point of view of nuclear structure. Namely, it has one proton and one neutron outside the doubly magic ^{4}He core, which makes it very suitable for studying the p-n interaction.

Experiment

Ion beam analysis set-up

The experiment was performed with the 2 MV Tandetron accelerator in the in-situ ion beam analysis (INSIBA) chamber [26,27,28] at Jožef Stefan Institute (JSI). The experimental setup is schematically shown in ref. [24]. The ^{3}He ion beam was oriented perpendicularly to the sample surface. Particles produced in the nuclear reaction are detected by a thick silicon detector (called NRA detector) with a depletion thickness of 1.5 mm. The detector had a circular aperture with a diameter of 19.54 mm and was positioned 104 mm from the target. The geometrical solid angle of the detector was 26.69 msr ± 0.12 msr. The detector efficiency and the solid angle were deduced by measuring the α-particle yield coming from a ^{241}Am source with known activity. To stop the back-scattered ^{3}He beam, a 24 μm thick Al absorber foil was placed in front of the NRA detector. The detector was positioned at the angles of 125°, 135° and 155° with respect to the incoming beam. The size of the beam spot on the target was defined by two consecutive circular orifices of 2 mm in diameter, positioned in the beam line. We also employed another detector for backscattered particles, the so-called Rutherford backscattering spectroscopy (RBS) detector. The depletion thickness of this detector was 300 μm. It was located 135 mm from the target at an angle of 165° with respect to the incoming beam covering a geometrical solid angle of 0.7 msr ± 0.02 msr. The backscattered signal from the ^{3}He ion beam on the Si wafer and the thin Pd and Ti layers measured by the RBS detector served us for determination of the absolute dose of ^{3}He particles impacting the samples. The beam current was measured by the ion mesh charge collector with a 77.4 % geometrical transmission [29] and a bias of 600 V. The uncertainty in the current measurement is about 4 %.

Samples were mounted on a sample holder which can hold up to 20 samples at the same time. For the energy calibration of the NRA detector, we used a deuterium-containing target consisting of dense, plasma-deposited thin amorphous deuterated hydrocarbon (a-C:D) film grown on a single crystal silicon (1 0 0) substrate. The thickness of the film was 275 nm, as measured with tactile profilometry. The ^{2}H/(C + ^{2}H) ratio was assumed to be about 0.34 consistent with a-C:H films deposited under the same conditions [30]. In the NRA spectrum measured on the a-C:D sample, the dominant signal is due to energetic protons from the ^{2}H(^{3}He,p)^{4}He, ^{12}C(^{3}He,p$_x$)^{14}N and ^{28}Si(^{3}He,p$_x$)^{30}P reactions that reach the detector. For energy calibration of the NRA detector, we have used the ^{2}H(^{3}He,p)^{4}He, ^{12}C(^{3}He,p$_1$)^{14}N and ^{12}C(^{3}He,p$_2$)^{14}N nuclear reactions with proton energies of 12.7 MeV 5.5 MeV and 3.3 MeV at 2.56 MeV ^{3}He energy at an angle of 125°. The energy calibration of the RBS detector was performed by measuring backscattered-particle energy spectra on multiple thick mono-elemental solid targets (Ta, Cu, Ti).

To obtain the ^{2}H concentration [31] in the deuterated PdTi layer sample, the proton signal from the ^{2}H(^{3}He,p)^{4}He nuclear reaction was measured at several ^{3}He energies (730, 1040, and 2570 keV) and the proton energy spectra were fitted by the SIMNRA simulation tool, version 7.02 [32].

To develop the NRA method using the ^{3}He beam and to determine the ^{3}H + ^{3}He → ^{4}He + ^{2}H and ^{3}H + ^{3}He → ^{5}He + ^{1}H cross-sections we measured the reaction yields of deuterons and protons. The cross-section measurements were performed with the ^{3}He energy range between 630 keV and 4300 keV. At energies above 2.5 MeV doubly charged ^{3}He ions were used to reach the higher energies. The applied analysing dose was 8.6 μC for energies ≤ 2500 keV and 4.3 μC for energies > 2500 keV. The background signal was measured on the PdTi layer loaded by ^{2}H$_2$ gas since there is some signal due to nuclear reaction between ^{3}He and Si in that energy range. Any possible change in the sample composition due to probing ^{3}He beam was checked by remeasuring the signal at the starting energy and no change in the film composition was observed.

To identify the reaction channels of interest in the measured energy spectra, we used a ΔE–E telescope detector placed at the angle of 135° with respect to the beam direction. The telescope detector consists of a 300 μm thick silicon detector backed by a 1 cm thick germanium detector placed in a common cryostat that cools both detectors to liquid nitrogen temperature. The detector was placed 11 cm from the target and the charged particle detection efficiency was 4.1x10^{-4}.

In addition, acceleration voltage was calibrated by using the following nuclear reactions: i) $^{27}Al(p,\gamma)^{28}Si$ [33], which has a sharp resonance at the beam energy of 991.86 keV; ii) The $^{19}F(p,\alpha\gamma)^{16}O$ nuclear reaction [34] with a sharp resonance at 340.46 keV; iii) The $^{1}H(^{19}F,\alpha\gamma)^{16}O$ nuclear reaction in inverse kinematics with a sharp resonance at the beam energy of 6421.5 keV. The final error of the calibrated ion-beam absolute energy was below 1 keV.

Sample preparation

The sample was prepared by depositing thin layers of Ti and Pd by a triode sputtering device on a 0.25 mm thick Si (1 0 0) wafer at JSI. Before the layer deposition, the Si wafer was heated to 130 °C in order to reach the working temperature and to ensure degassing of adhered water. The vacuum was enhanced by gettering, i.e. sputtering of a titanium target on a shutter for 10 min. After that, the shutter was removed and the titanium target was sputtered for an additional 5 min at the conditions 1700 V × 0.6 A. The typical deposition rate for titanium at these conditions is 11 nm/min, meaning that the deposited titanium layer is expected to be about 55 nm thick. After that, a palladium target was sputtered. The chosen sputtering conditions are somewhat different due to material properties (1200 V × 0.4 A). The sputtering lasted 10 min at an estimated deposition rate of 1.4 nm/min. It is expected that these sputtering conditions would give a 14 nm thick layer of palladium. However, due to start-up and shutdown effects, the thickness is likely different. The real composition of layers was analysed by RBS simultaneously with the NRA measurements using a ^{3}He beam. We have chosen for this material composition since is well-known that Ti is a hydrogen getter [35]. The use of Pd was decided due to the fact that Pd acts as a catalyst for hydrogen molecule dissociation on the surface and can prevent Ti oxidation [8]. We have prepared previously a test Ti layer on a Si wafer without the Pd layer on top and we did not observe any deuterium uptake in the Ti layer.

One Si wafer of Ti covered by Pd layer was then cleaved into smaller pieces with dimensions of approximately 5 × 10 mm^2. Each cut sample could then experience different hydrogen isotope loading procedures performed at Saclay Tritium Lab, belonging to the French Alternative Energies and Atomic Energy Commission (CEA). A successful loading procedure was developed with deuterium gas at 1.8 × 10^5 Pa at different temperatures of 200 °C, 300 °C and 400 °C. The success of the loading procedure was tested by the ^{3}He NRA method at the JSI. The trapping of deuterium was successful at all temperatures. The protocol that is used is divided into two steps. In the first step, the sample is exposed to $^{1}H_2$ atmosphere (99.9992 %) at 300 ± 2 °C and (1.55 ± 0.05) × 10^5 Pa. During this step, the uptake of hydrogen into the titanium bulk is initialized. The palladium promotes the hydrogen uptake on titanium preventing and limiting the formation of titanium oxide acting like a barrier for hydrogen isotope absorption. Moreover, traces of water are removed thanks to a CO_2 cold trap at −79.5 °C. In the second step, the sample is exposed to the labelling isotope ($^{2}H_2$ or $^{3}H_2$ at 99 % of isotopic enrichment) gas atmosphere in a sealed glass tube. The treatment lasts 1 h at 300 ± 2 °C and above (1.55 ± 0.05) × 10^5 Pa. According to the protocol, two fresh samples were loaded with $^{3}H_2$ gas at 300 °C and 1.6 × 10^5 Pa for 1 h. The sample is placed in an airtight container and is swept by the non-contaminated airflow. Tritium release from the sample is then trapped in the feeding bottles of a tritium bubbler (MARC 7000 from SDEC France 2010). As, tritium release was detected at room temperature after many days, an annealing procedure was performed: the sample was heated to 100 °C to remove the loosely bound tritium that would migrate at room temperature and to guarantee zero release of tritium during transport and NRA experiments. One of the two samples was sent to JSI for cross-section analysis. The second one was used to determine the total ^{3}H activity by liquid scintillation counting technique using a Tri-Carb 2910TR analyser from Perkin-Elmer. The coupling of the heating system with the airtight tank and the bubbler allows forced outgassing of tritium from the sample. The total activity is accumulated in the bubbler after a 4 h step at 200 °C (Fig. 1) and measured by liquid scintillation. Another step followed with an increasing temperature from 200 °C to 800 °C to control the end of the release. Tritium release was checked by rapid annealing to 1000 °C and no increase in release activity was observed. After 15 h of cooling down (the furnace temperature decreases slowly), there was still no increase in the release activity from the sample. Finally, the sample was checked with a surface contamination meter (LB123 from Berthold Technologies). The intensity of the signal was less than two times the background noise. This means sufficiently low to neglect a small amount that could be trapped in the sample compared to the uncertainty of the measurements. The total amount of tritium activity measured after such procedure was 270 MBq for a sample with an area of 53.3 mm^2 which lead to 395 ± 59 MBq for a sample with an area of 77.96 mm^2 (11.3 × 6.9 mm^2) studied by NRA.

The individual layer thicknesses were determined with the RBS measurements. The PdTi layer consists of (115 ± 6) × 10^{15} Pd atoms/cm^2 corresponding to 17 nm of Pd on top of (335 ± 10) × 10^{15} Ti atoms/cm^2 corresponding to approximately 59 nm of Ti, deposited on a Si wafer. For the first trial of the loading procedure, we measured the ^{2}H amount by NRA in deuterated samples that were exposed to $^{2}H_2$ gas at different temperatures. In this case, the NRA detector was positioned at 160°. In the deuterated sample loaded at 200 °C, we obtained (380 ± 10) × 10^{15} $^{2}H/cm^2$ corresponding to 53 at.% $^{2}H/(^{2}H + Ti)$ assuming that ^{2}H only stayed in the Ti layer. Since our deuterium depth resolution at the surface is 100 nm [36], we were not able to determine whether the deuterium was trapped only in the Ti layer or also in the Pd layer. For the sample loaded at 300 °C we got (390 ± 10) × 10^{15} $^{2}H/cm^2$ corresponding to 54 at.% $^{2}H/(^{2}H + Ti)$ and in the 400 °C loaded sample we obtained (270 ± 15) × 10^{15} $^{2}H/cm^2$, which corresponds to 42 at.%. The tritiated sample prepared for cross-section measurements had the dimensions of 11.3 × 6.9 mm^2 which corresponds to an activity of 395 ± 59 MBq. This results in 2.22 × 10^{17} ^{3}H atoms. Considering the surface area of the sample is 0.78 cm^2, one obtains (285 ± 43) × 10^{15} $^{3}H/cm^2$ which corresponds to (46 ± 7) at. % of tritium in the Ti layer. This is within the error bars in good agreement with the amount of ^{2}H measured in the deuterated PdTi-Si samples.

Results

A comparison of the NRA spectra obtained with ^{3}He at an energy of 2.5 MeV on deuterated PdTi-Si, tritiated PdTi-Si and a-C:D samples is shown in Fig. 2. The spectra were measured at an angle of 125° in the laboratory system. The peak at the highest energies of about 12.5 MeV comes from the nuclear reaction of ^{3}He with deuterium in the samples. At energies lower than 6 MeV there are three peaks coming from the nuclear reaction of ^{3}He with ^{12}C. In the energy region between 6 and 9 MeV the two distinct peaks can be clearly seen that correspond to the channels (1) and (3) defined in the Introduction, of the $^{3}He+^{3}H$ nuclear

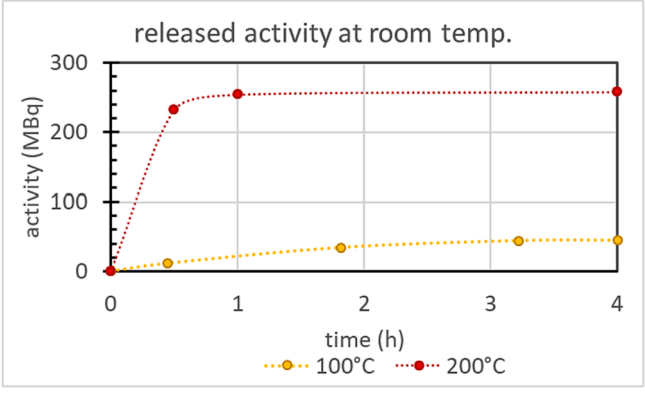

Fig. 1. Measurement of the activity of the tritiated PdTi-Si sample with 53.3 mm^2 after annealing at 100 °C and outgassing at 200 °C of a sample.

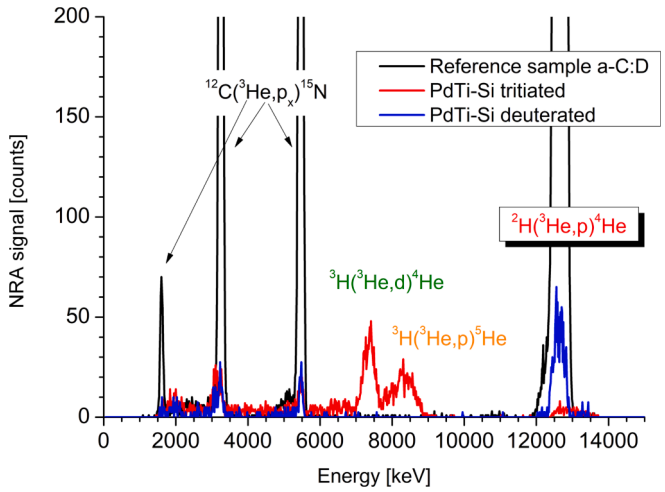

Fig. 2. Spectra from the tritiated PdTi-Si (red), deuterated PdTi-Si (blue) and a-C:D (black) samples measured with NRA detector placed at an angle of 125° and the ^{3}He beam with an energy of 2.5 MeV. (For interpretation of the references to colour in this figure legend, the reader is referred to the web version of this article.)

reactions.

Cross-section determination on thin solid target

The ^{3}He+^{3}H yields measured by the NRA detector (with summed contributions of both tritium-related peaks) as a function of ^{3}He energy measured at three different scattering angles are shown in Fig. 3. The NRA signal from the tritiated PdTi-Si sample was subtracted by the background measured in the same energy range on the deuterated PdTi-Si sample. The yield is the highest for the lowest measured angle which agrees well with the measurements by Nocken [22]. The signal increases with the ^{3}He energy for all three angles.

For the differentiation of the two peaks observed in Fig. 2 we utilized the ΔE–E telescope detector. Since the deuterons from the ^{3}He+^{3}H reaction are stopped in the silicon detector, while the protons from the same reaction pass through the first detector and are stopped by the germanium detector, we were able to determine that the first peak is due to channel (1) and the high energy peak is due to channel (3). The continuous energy protons from the channel (2) lie beneath the carbon background. The signal obtained by this detector is shown in Fig. 4.

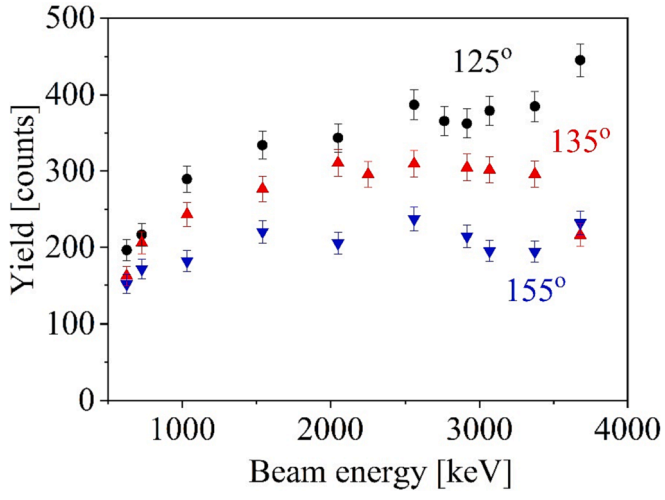

Fig. 3. NRA yield from channel (1) and (3) together as a function of the ^{3}He beam energy measured at three different scattering angles.

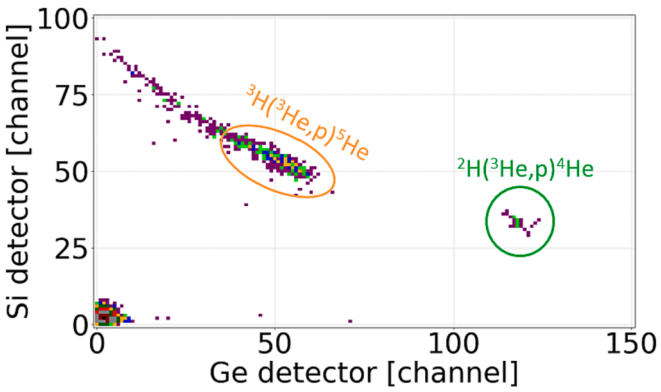

Fig. 4. NRA yield as measured with the ΔE–E detector, shown as a two-dimensional plot of the germanium detector signal on x axis vs. the silicon detector signal on y axis. Only the protons pass through the silicon detector, so the green circle marks the protons from the ^{2}H(^{3}He,p)^{4}He reaction, while the orange area marks the protons from channels (2) and (3) of the reaction on tritium. The ^{3}He beam energy was 1 MeV. (For interpretation of the references to colour in this figure legend, the reader is referred to the web version of this article.)

Since the depth resolution of NRA measurement for deuterium detection at the surface is between 100 and 300 nm [36], depending on the scattering angle, we were not able to determine whether the deuterium was trapped only in the Ti layer or also in the Pd layer. Assuming that all the tritium is trapped in the Ti layer, the ^{3}He beam loses some energy in the Pd layer. This energy loss, according to SRIM tables [37], calculated by the SIMNRA program, is between 12.9 keV and 6.8 keV at ^{3}He ion beam energies from 0.63 MeV to 3.3 MeV, respectively. The cross-section energy is determined in the middle of the Ti layer which corresponds to an additional energy loss in one half of the Ti layer being 16.4 keV and 7.8 keV for ^{3}He energies between 0.63 MeV and 3.3 MeV, respectively.

The cross-section for the channel (1) was determined by integrating the signal of the first peak, subtracting the background, and dividing it by the solid angle, beam dose and the above-determined amount of tritium in the sample. The cross-section was rechecked by inserting its value into the r33 file and fitting the number of counts in the energy spectrum under the peak with the Gaussian function using the SIMNRA software [32] and subtracting the background in the corresponding energy region. Regarding the channel (3), the ground state of the ^{5}He nucleus is broad ($\Gamma = 0.648$ MeV [38,39] meaning that the energy distribution of the protons emitted from this channel will also be broad. Since SIMNRA does not consider the state widths for the energy distribution simulations, the signal from the channel (3) could not be properly fitted using SIMNRA software. So, the cross-section for the channel (3) was calculated by subtracting the total number of counts under both peaks (corrected for the background) from the number of counts under the first peak. However, since the tail of the peak coming from the channel (3) is spread under the peak belonging to the channel (1), this will introduce a certain uncertainty in the resulting cross-sections of both channels. The obtained differential cross-sections measured at 135° determined individually for the channel (1) denoted as "^{4}He + d" and channel (3) denoted as "^{5}He + p" are shown in Fig. 5. We compare also the cross-sections measured by Kuhn et al. [21], Nocken et al. [22] and Nam et al. [25]. In the energy range where we have some overlap with the present study, we have excellent agreement with Kuhn et al. and very good agreement with the other two literature data. The data by Nam et al. [25] are slightly higher than the present data, but it needs to be noted that the scattering angle in that case was 133° ± 1° except for the data point for the lowest energy. There it was measured at 138° and this data point is slightly lower than our data. This indicates that there might be a strong angular dependence, which will be shown in the

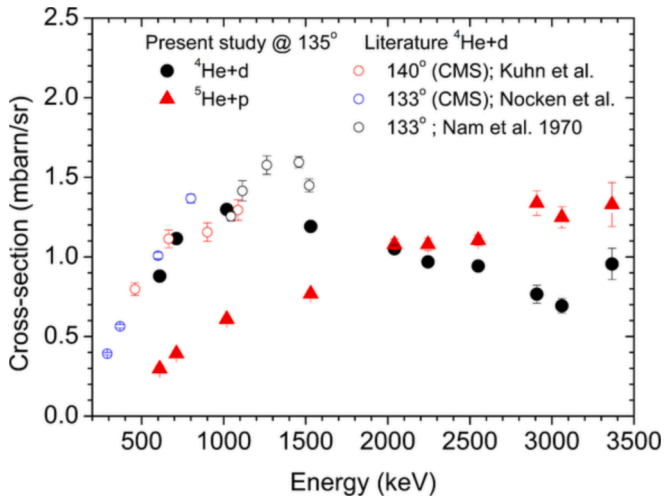

Fig. 5. Differential cross-sections determined at the scattering angle of 135° separately for channel (1), marked as "^{4}He + d", and channel (3), marked as "^{5}He + p". For comparison we also show the cross-sections measured by Kuhn et al. [21], Nocken et al. [22] and Nam et al. [25].

following.

In Fig. 6, the differential cross-sections at the 125° and 155° scattering angles are shown. We can see that the shape of the cross-sections is similar for all three angles only the absolute value is higher at the lower angle and vice versa. The cross-sections from the present study are compared to the literature [25] and the agreement is very good, especially at 155°. The cross-section from Nam et al. [25] is higher than ours measured at 125° but this could be again due to a slightly lower angle in [25] (122° ± 1°), except for the first data point that was measured at 128° and in that case the cross section is slightly lower. The same was observed when we compared the cross-sections measured at 135°. The errors bars shown in Figs. 5 and 6 are due to the statistics of the measurements. Additionally, we have to consider that we have a systematic error of 5 % due to the current measurement and the solid angle determination. To this one needs to add the uncertainty of the tritium quantity in the sample, which accounts for 15 %. The total uncertainty is the square root of the quadratic sum of all individual error bars as they are independent of each other. The tables of differential cross-section data with total uncertainty for all measured angles are given in Supplementary file.

We have not observed any sign of the $J^\pi = 2^-$ broad resonance reported at 17985 keV excitation energy in [38,40,41]. This excitation energy in our case corresponds to a ^{3}He beam energy of 4.4 MeV. Instead, we observed that at this beam energy, many other reaction channels open for our target and the spectra become polluted. The cross-section behaves rather as expected for a non-resonant cross-section. The ^{3}He(^{3}H,d)^{4}He cross-section falls as the ^{3}He(^{3}H,p)^{5}He reaction probability increases at higher energies. The only possibility for the existence of this resonance is that it is built on the ground state of ^{5}He to which it preferentially decays. The main decay channel (^{4}He + d) is then suppressed. The odd proton would have to sit in the 1 $s_{1/2}$ (or 0$d_{5/2}$) orbit to couple with a 0$p_{3/2}$ neutron to $J^\pi = 2^-$. The excitation energy is then higher than expected from shell model calculations [42].

Angular distribution for the two channels at two energies of 1 MeV and 2.5 MeV were measured in an angular range between 105° and 165°, shown in Fig. 7. In this case, for each data point the detector was moved to a specific angle and the signal was measured on the tritiated and deuterated PdTi-Si samples. One can see that the cross-section for the channel (1) is decreasing with the angle. The cross-section dependence with the angle agrees with the measurements by Nocken et al. [22], showing that the cross-section attains its maximum at 90 degrees and drops for larger angles. We also compare the measured angular distribution for the channel (1) by Nam et al. [25] for 1 MeV and the agreement is very good. On the other hand, for channel (3) there is no

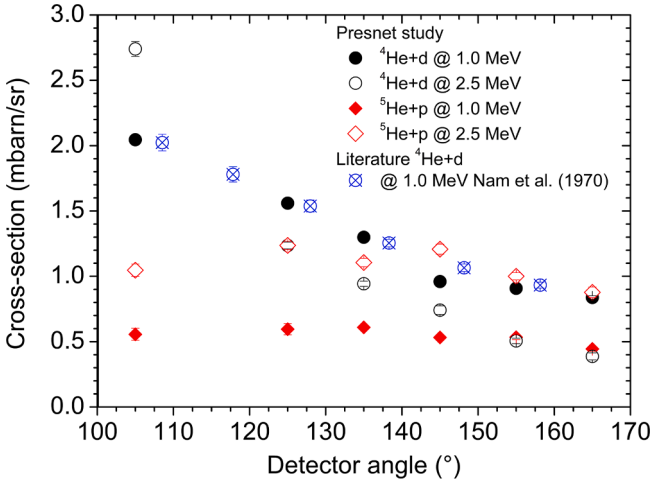

Fig. 7. Angular dependence of the differential cross-sections for channel (1), marked as "^{4}He + d", and channel (3), marked as "^{5}He + p", at two ^{3}He beam energies of 1 MeV and 2.5 MeV in laboratory system. Angular dependence as measured by Nam et al. [25] at 1 MeV is also shown.

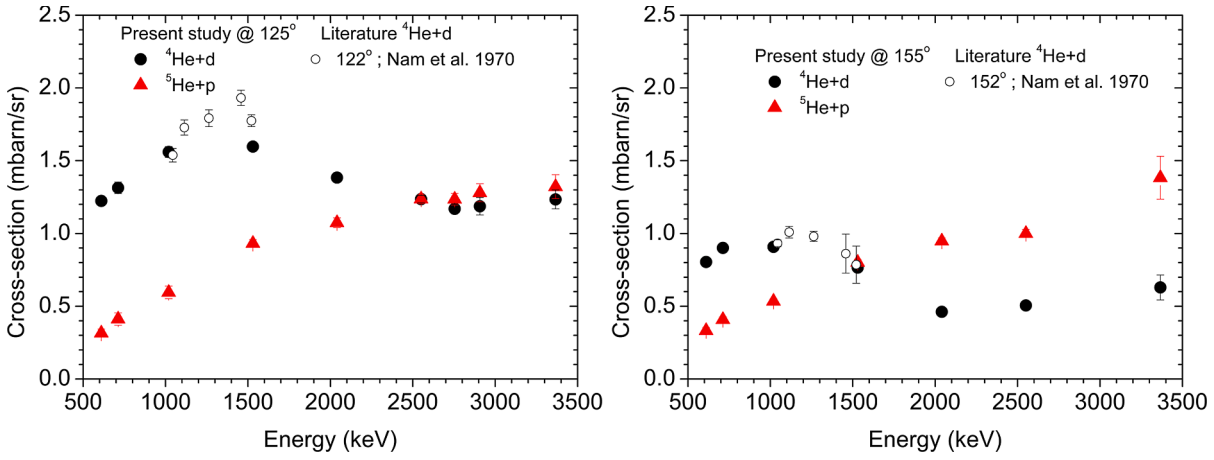

Fig. 6. Differential cross-section determined at scattering angles of 125° (left) and 155° (right) for reaction channel (1), marked as "^{4}He + d", and channel (3), marked as "^{5}He + p". For comparison we also show data from Nam et al. [25].

specific angular dependence especially at 1 MeV whereas at 2.5 MeV it slightly increases at 125° and then again decreases.

Application of cross-sections on thick solid target

The differential cross-sections measured at 135° were further verified on a thick tritiated solid tungsten target. For this purpose, a tungsten sample was first irradiated by 20 MeV W ions to create defects into which hydrogen isotope atoms can be trapped, as described in [27,24]. The sample was loaded at 450 °C by $^{3}H_2$ gas. The sample loading and measurement procedure is described in detail in [24]. The applied ^{3}He beam analysing dose was 34.2 μC for energies ≤ 2500 keV and 17.1 μC for energies > 2500 keV, which is four times higher dose than that used for the PdTi film. No outgassing during ^{3}He analysis is anticipated since deuterium is strongly trapped at defects in tungsten [43]. At most 6 % reduction of deuterium was measured on such samples after 1.5 years [44]. The experimental spectra obtained on that sample [24] were then fitted in the SIMNRA program [32] using the above-determined differential cross-sections at 135° by varying the tritium depth profile in the target. The obtained fits are shown in Fig. 8 for different ^{3}He energies. The tritium depth profile that gave the best fit to the spectra is shown in Fig. 9. With such a depth profile we managed to obtain a good agreement of the integral counts and the shape for the first narrow peak from reaction channel ^{3}H(^{3}He,d)^{4}He, for all energies. The different energies give information about the tritium depth profile at different depths. Namely, at higher ^{3}He energies we obtain the information from higher depths since the penetration of the beam is deeper.

We show in the Fig. 8 also the SIMNRA fitting result for the channel (3) which is ^{3}H(^{3}He,p)^{5}He. Contrary to the first one, the simulated right peak is not in good agreement with the measured spectra. This is mainly due to the fact that the resonance for this decay channel is very broad and therefore the energy distribution of the products is also broad. This means that the protons coming from that reaction have a larger energy distribution than is usually given from nuclear reaction channels. For this reason, the right peak was broadened by the width of the reaction and is shown additionally as a dashed line for individual energies. The sum of the first peak and the width-corrected peak is shown as a black line. The agreement of the corrected simulated spectra and the measurement is then very good.

Since we can still rather well distinguish the contribution from the

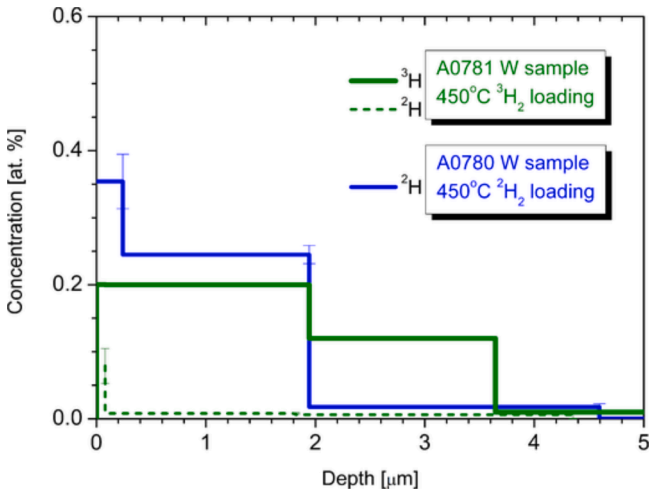

Fig. 9. The ^{3}H depth profile for the W self-damaged sample A0781 exposed to $^{3}H_2$ gas at 450 °C, olive line. This depth profile was used for the fitting of the spectra shown in Fig. 8. Dashed green shows the ^{2}H concentration in this sample. For comparison we also show the ^{2}H depth profile as obtained on the W self-damaged sample A0780 exposed to $^{2}H_2$ gas at 450 °C, blue line. (For interpretation of the references to colour in this figure legend, the reader is referred to the web version of this article.).

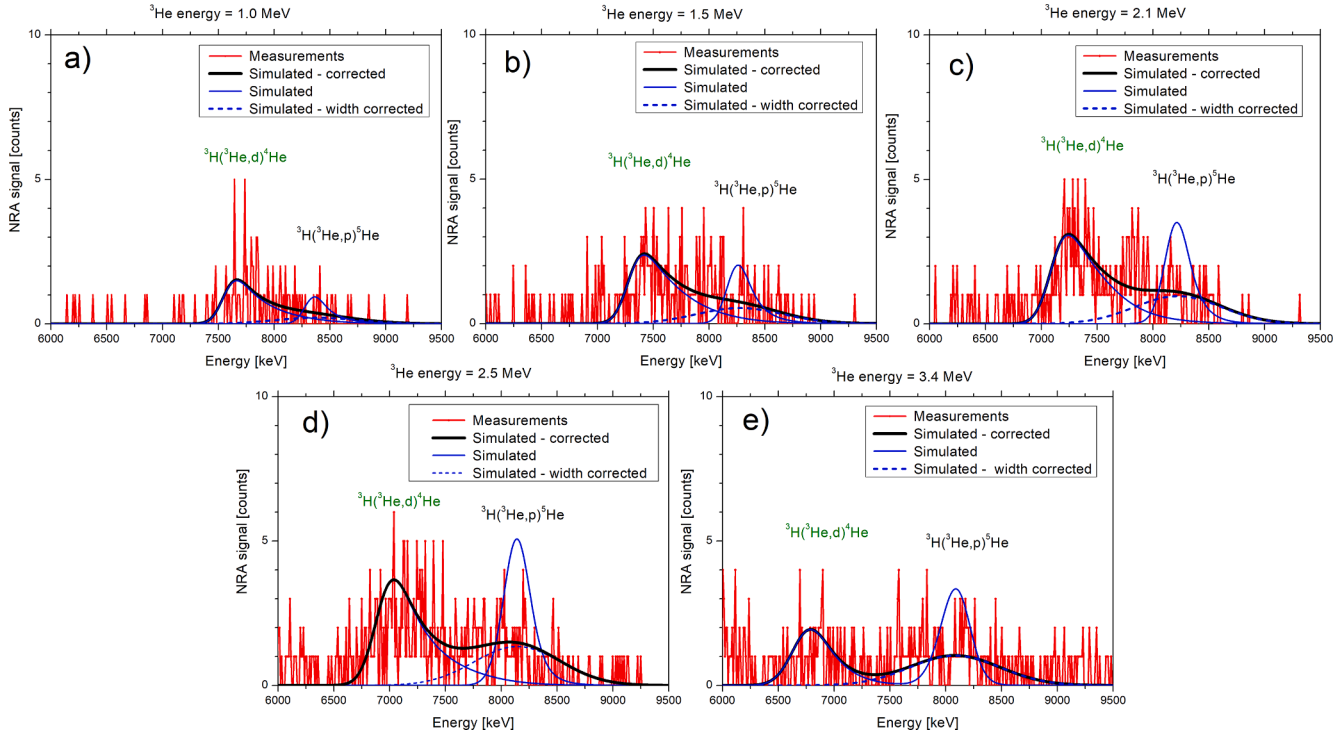

Fig. 8. Experimental spectra (red) measured at different primary ^{3}He ion energy from 1 MeV to 3.4 MeV at 135° together with the fitted spectrum (black) using the above determined differential cross-sections. The simulated spectra as obtained from SIMNRA (blue line), was for channel (3) corrected for the width of the reaction channel and is shown as a dashed blue line. This width-corrected spectrum is then summed together with the spectrum for channel (1), shown as a black line. (For interpretation of the references to colour in this figure legend, the reader is referred to the web version of this article.). (For interpretation of the references to colour in this figure legend, the reader is referred to the web version of this article.)

two decay channels, we were able to determine the tritium depth profile by fitting the first peak from the channel (1). The ^{3}H depth shown in Fig. 9 is compared to the ^{2}H depth profile obtained on a sample that was loaded by $^{2}H_2$ gas in the same way as the tritiated sample. Both samples were irradiated by 20 MeV W ions that create displacement damage down to 2.3 μm where hydrogen isotopes are effectively trapped. The ^{2}H and ^{3}H concentrations are in good agreement within this damaged depth, showing a homogeneous ^{2}H and ^{3}H concentration of 0.20 at. % for ^{3}H and 0.25 at. % for ^{2}H from 0.2 μm down to 2 μm. The tritiated sample beyond 2 μm attains 0.12 at. % down to 3.6 μm and then decreases to 0.001 at. % which is the level that we typically observe on unirradiated polycrystalline W [27]. The difference between ^{3}H and ^{2}H concentrations in this second layer from 2 to 3.6 μm could be due to the poorer depth resolution for ^{3}H or the uncertainty in the signal fit due to the background from channels (2) and (3), which becomes higher at higher ^{3}He energies. The ^{3}H concentration below 3 μm is not easy to determine since an overlap exists with the signal from the channel (3). Since the cross-section for the channel (1) has no sharp resonance and is almost constant over the measured energy range, this means that we are similarly sensitive at all analysing depths. Therefore, the distribution of the measured signal at a given energy gives us the informative distribution of the tritium in the sample. Varying the energy only changes the depth to which we can still obtain information about the ^{3}H concentration. Therefore, by measuring at 2.5 MeV beam energy, we obtain information about the amount of ^{3}H down to about 3.5 μm. Measurements at higher energies will not give us with any additional information because the signal from higher depths is in the energy range where we have an overlap with the signal from the channel (3) and therefore we cannot determine the ^{3}H concentration with high accuracy.

Conclusion

We have measured and evaluated differential cross-sections for two decay channels for the nuclear reaction between ^{3}He and ^{3}H in the energy range between 0.6 MeV and 3.4 MeV. The cross-sections were measured at three different scattering angles 125, 135 and 155°. The evaluated cross-section was compared with the cross-section determined by Nocken et al. [22], Kuhn et al. [21] and Nam et al. [25] and good agreement was found with the present measured cross-section. With the obtained cross-sections we have evaluated the ^{3}H depth profile on a thick tungsten target measured in [24]. We have fitted the measured spectra for the channel (1) by changing the ^{3}H distribution in the sample. The obtained ^{3}H depth profile is in good agreement with the deuterium depth profile on a sample that experienced the same irradiation and loading procedure, but with a $^{2}H_2$ exposure gas. We estimated that with the present differential cross-section data we can obtain ^{3}H depth profile information down to 3.5 μm in tungsten. Beyond this depth, the signal from the channel (1) overlaps with the signal from the channel (3), which has a broad energy distribution and cannot give us reliable information about the ^{3}H depth profile.

CRediT authorship contribution statement

S. Markelj: Writing – review & editing, Writing – original draft, Visualization, Resources, Investigation, Formal analysis, Conceptualization. **A. Cvetinović:** Writing – review & editing, Investigation, Formal analysis. **M. Lipoglavšek:** Writing – review & editing, Investigation, Conceptualization. **M. Kelemen:** Writing – review & editing, Investigation. **M. Čekada:** Writing – review & editing, Investigation. **P. Pelicon:** Resources. **M. Payet:** Writing – review & editing, Investigation. **C. Grisolia:** Writing – review & editing, Resources.

Declaration of competing interest

The authors declare that they have no known competing financial interests or personal relationships that could have appeared to influence the work reported in this paper.

Data availability

Data will be made available on request.

Acknowledgments

The authors would like to acknowledge dr. Thomas Schwarz-Selinger from Max-Planck Institut for Plasma Physics for preparation of the a-C:D films.

This work was carried out within the TRANSAT project that received funding from the Euratom research and training programme 2014-2018 under grant agreement N° 754586.

This work was supported by IAEA Coordinated Research Project F11023, entitled 'Development and Application of Ion Beam Techniques for Materials Irradiation and Characterization relevant to Fusion Technology'.

This work was supported by the project TITANS, that is funded by the European Union. Views and opinions expressed are however those of the author(s) only and do not necessarily reflect those of the European Union or the European Atomic Energy Community ('EC-Euratom'). Neither the European Union nor the granting authority can be held responsible for them.

Appendix A. Supplementary data

Supplementary data to this article can be found online at https://doi.org/10.1016/j.nme.2024.101586.

References

[1] J. Bøttiger, A review on depth profiling of hydrogen and helium isotopes within the near-surface region of solids by use of ion beams, J. Nucl. Mater. 78 (1978) 161–181.
[2] M. Rubel, D. Primetzhofer, P. Petersson, S. Charisopoulos, A. Widdowson, Accelerator techniques and nuclear data needs for ion beam analysis of wall materials in controlled fusion devices, EPJ Techn Instrum 10 (2023) 1–21.
[3] J. Sawicki, Tritium implantation and depth profiling in fusion related materials, Nucl. Instr. Meth. Phys. Res. B 23 (1987) 521.
[4] J. Sawicki, Measurements of the differential cross sections for recoil tritons in 4He-3T scattering at energies between 0.5 and 2.5 MeV, Nucl. Inst. Meth. Phys. Res B 30 (1988) 123.
[5] M. Wilde, K. Fukutani, Hydrogen detection near surfaces and shallow interfaces with resonant nuclear reaction analysis, Surf. Sci. Rep. 69 (2014) 196–295.
[6] A. Jaffe, F. d. S. Barros, P. Forsyth, J. Muto, I. Taylor and S. Ramavataram, Some (t, p) Reactions in Light Nuclei, Proc. Phys. Soc. 76 (1960) 914–928.
[7] I. Bykov, P. Petersson, H. Bergsåker, A. Hallén, G. Possnert, Investigation of tritium analysis methods for ion microbeam application, Nucl. Inst. Methods Phys. Res. B 273 (2012) 250–253.
[8] X. Xia, W. Ding, B. Zhang, X. Long, S. Luo, S. Peng, R. Hutton, L. Shi, Cross-section for proton–tritium scattering from 1.4 to 3.4MeV at the laboratory angle of 165°, Nucl. Inst. Methods Phys. Res. B 266 (2008) 705.
[9] J.C. Davis, J.D. Anderson, Tritium depth profiling by neutron time−of−flight, J. Vac. Sci. Technol. 12 (1975) 358–360.
[10] M. Caterini, D. Thompson, P. Wan, J. Sawicki, Tritium profiling using the T(d, 4He) n reaction, Nucl. Instrum. Methods Phys. Res., Sect. B 15 (1986) 535–539.
[11] S. Okuda, R. Taniguchi, M. Fujishiro, Tritium depth profiling in surface regions of solids by the use of the T(d, a)n reaction, Nucl. Instr. Meth. Phys. Res. B 14 (1986) 304.
[12] C. Stan-Sion, et al., Tritium retention measurements by accelerator mass spectrometry and full combustion of W-coated and uncoated CFC tiles from the JET divertor, Nucl. Fusion 56 (2016) 046015.
[13] E. Pajuste, et al., Structure, tritium depth profile and desorption from 'plasma-facing' beryllium materials of ITER-Like-Wall at JET, Nucl. Mater. Energy 12 (2017) 642–647.
[14] V.K. Alimov, Y. Torikai, Y. Hatano, T. Schwarz-Selinger, Tritium retention in displacement-damaged tungsten exposed to deuterium-tritium gas mixture at elevated temperatures, Fusion Eng. Des. 162 (2021) 112100.
[15] V. Alimov, M. Mayer, J. Roth, Differential cross-section of the D(3He, p)4He nuclear reaction and depth profiling of deuterium up to large depths, Nucl. Instr. and Meth. in Phys. Res. B, 234, 2005.
[16] B. Wielunska, M. Mayer, T. Schwarz-Selinger, U. von Toussaint and J. Bauer, "Cross Section Data for the D(3He,p)4He Nuclear Reaction from 0.25 to 6MeV," Nucl. Instr. and Meth. in Phys. Res. B, vol. 371, p. 61, 2016.

[17] S. Möller, Analytical continuous slowing down model for nuclear reaction cross-section measurements by exploitation of stopping for projectile energy scanning and results for 13 C(3 He,α) 12 C and 13 C(3 He,p) 15 N., Nucl. Instr,. Meth. Phys. Res. B, vol. 394 , p. 134–140 , 2017.
[18] M. Guitart Corominas, T. Schwarz-Selinger, Experimental determination of the 16O (3He, p0)18F differential cross section, Nucl. Instrum. Methods Phys. Res., Sect. B 450 (2019) 13–18.
[19] N.P. Barradas, et al., Determination of the 9Be(3He,pi)11B (i = 0,1,2,3) cross section at 135° in the energy range 1–2.5 MeV, Nuclear Instruments and Methods in Physics Research Section B: Beam Interactions with Materials and Atoms, 346, p. 21, 2015.
[20] C. Moak, A Study of the H 3+ He 3 Reactions, Phys. Rev. 92 (1953) 383.
[21] B. Kühn, B. Schlenk, Winkelverteilungen für die reaktion He3 + T, Nucl. Phys. 48 (1963) 353.
[22] U. Nocken, U. Quast, A. Richter, G. Schrieder, The reaction 3H(3He, d)4He at very low energies: Energy dependent violations of the Barshay-Temmerisospin theorem and highly excited states in 6Li, Nucl. Phys. A 213 (1973) 97–106.
[23] M. Wang, G. Audi, F. Kondev, W. Huang, S. Naimi, X. Xu, The AME2016 atomic mass evaluation (II). Tables, graphs and references, Chinese Phys. C 41 (2017) 030003.
[24] S. Markelj, et al., Tritium measurements by nuclear reaction analysis using 3He beam in the energy range between 0.7 MeV and 5.1 MeV, Nucl. Mater. Energy 28 (2021) 101057.
[25] K. Nam, G. Osetinskii, V. Sergeev, Isospin Conservation in the Reaction He3(t, d) He4, Soviet J. Nucl. Phys. 10 (1970) 407.
[26] M. Mayer, e. al.,, Ion beam analysis of fusion plasma-facing materials and components: facilities and research challenges, Nucl. Fusion 60 (2020) 025001.
[27] S. Markelj, A. Založnik, T. Schwarz-Selinger, O.V. Ogorodnikova, P. Vavpetič, P. Pelicon, I. Čadež, In situ NRA study of hydrogen isotope exchange in self-ion damaged tungsten exposed to neutral atoms, J. Nucl. Mater. 469 (2016) 133–144.
[28] A. Založnik, P. Pelicon, Z. Rupnik, I. Čadež and S. Markelj, "In situ hydrogen isotope detection by ion beam methods ERDA and NRA," Nucl. Instr. and Meth. in Phys. Res. B, vol. 371, p. 167, 2016.
[29] M.E. Bouanani, P. Pelicon, A. Razpet, I. Cadez, M. Budnar, J. Simcic, S. Markelj, Nucl. Inst. Meth. Phys. Res. B 243 (2005) 392.
[30] T. Schwarz-Selinger, A. von Keudell, W. Jacob, Plasma chemical vapor deposition of hydrocarbon films: The influence of hydrocarbon source gas on the film properties, J. Appl. Phys. 86 (1999) 3988.
[31] M. Mayer, E. Gauthier, S. K, U.v. Toussaint, Nucl. Instr. Meth. Phys. Res. B 267 (2009) 506.
[32] M. Meyer, "SIMNRA User's Guide, Report IPP 9/113," Max-Planck-Instutut für Plasmaphysik, Garching, Germany, Available: http://www.rzg.mpg.de/~mam/., 1997.
[33] K. Spyron, et al., Eur. Phys. J. A 7 (2000) 79.
[34] S. Harissopulos, et al., Eur. Phys J. A9 (2000) 479.
[35] Y. Fukai, The Metal-Hydrogen systems, Springer-Verlag, Berlin Heidelberg, 2005.
[36] S. Markelj, et al., Deuterium transport and retention in the bulk of tungsten containing helium: the effect of helium concentration and microstructure, Nucl. Fusion 60 (2020) 106029.
[37] J. Ziegler, "www.srim.org.," [Online].
[38] X. Hu, et al., Nucl. Physics A708 (2002) 3.
[39] D.R. Tilley, et al., Energy levels of light nuclei A=5, 6, 7, Nucl. Phys. A 708 (2002) 3.
[40] G. Schrieder, H. Genz, A. Richter, W. Von Witsch, Neutron-proton final state interaction in the 3H(3He, pα)n reaction at low bombarding energies, Nucl. Phys. A 247 (1975) 203–210.
[41] G.J. Wagner, C.C. Foster, B. Greenebaum, Apparent violation of isospin symmetry in the reaction 2H(α, t)3He near threshold, Nucl. Phys. A 174 (1971) 123–128.
[42] D. Zheng, et al., Phys. Rev. C 52 (1995) 2488.
[43] E.A. Hodille, A. Založnik, S. Markelj, T. Schwarz-Selinger, C.S. Becquart, R. Bisson, C. Grisolia, Simulations of atomic deuterium exposure in self-damaged tungsten, Nucl. Fusion 57 (2017) 056002.
[44] B. Wielunska, M. Mayer, T. Schwarz-Selinger, A.E. Sand, W. Jacob, Deuterium retention in tungsten irradiated by different ions, Nucl. Fusion 60 (2020) 096002.